

FABRICATION AND ELECTRICAL PROPERTIES OF $\text{Li}_3\text{Sc}_{2-x}\text{B}_x(\text{PO}_4)_3$ SUPERIONIC MATERIALS*

T. Šalkus^a, E. Kazakevičius^a, V. Kunigėlis^a, L. Jucius^a, A. Dindune^b, Z. Kanepe^b,
J. Ronis^b, A. Kežionis^a, B. Bleiber^d, H.-J. Lang^c, and A.F. Orliukas^a

^a Faculty of Physics, Vilnius University, Saulėtekio 9, LT-10220 Vilnius, Lithuania

E-mail: antanas.orliukas@ff.vu.lt

^b Institute of Inorganic Chemistry, Riga Technical University, Miera 34, LV-2169 Salaspils, Latvia

^c Institute of Ceramic Materials, Freiberg University of Mining and Technology, Gustav-Zeuner-Str. 3, D-09596 Freiberg, Germany

^d Institute of Physical Metallurgy, Freiberg University of Mining and Technology, Gustav-Zeuner-Str. 5, D-09599 Freiberg, Germany

Received 17 June 2005

The $\text{Li}_3\text{Sc}_{2-x}\text{B}_x(\text{PO}_4)_3$ compounds, with $x = 0-2$, were synthesized by a solid state reaction and studied by X-rays. The ceramic samples were sintered and studied by digital scanning microscope. The electrical properties of the ceramic ($x = 0, 0.5, 1$) and glass ($x = 2$) samples were investigated in a frequency range $10^6-1.2 \cdot 10^9$ Hz and in a temperature range 300–600 K. Two regions of relaxational dispersion were found in conductivity spectra of the ceramics. They are related to the fast Li^+ ion transport in the bulk and in the grain boundaries of the ceramics. Isomorphous substitution $\text{Sc} \rightarrow \text{B}$ leads to a change of temperature of the phase transition to γ -phase (T_γ). The increase of stoichiometric factor x caused the increases of intragrain (σ_g) and total (σ_{tot}) conductivities, and also the decrease of their activation energies in the temperature range below T_γ .

Keywords: solid electrolyte ceramics, superionic ceramics, fast ion transport, ionic conductivity

PACS: 61.10.Nz, 66.30.Hs, 81.05.Je, 82.45.Yz

1. Introduction

It is known that two structural phase transitions take place in $\text{Li}_3\text{Sc}_2(\text{PO}_4)_3$ crystals in temperature range from 293 to 573 K [1, 2]. The phase transitions are caused by order–disorder processes in the lithium sublattice. The $\text{Li}_3\text{Sc}_2(\text{PO}_4)_3$ compound at room temperature (α -phase) and at $T = 473$ K (β -phase) belongs to a monoclinic crystallographic system (s. g. $P2_1/n$), however, at $T = 573$ K (γ -phase) the crystals belong to the rhombic spatial symmetry group $Pcan$ [2, 3]. In the γ -phase the lithium sublattice is disordered the most and the γ - $\text{Li}_3\text{Sc}_2(\text{PO}_4)_3$ crystals are solid electrolytes with fast Li^+ ion transport [2, 4]. The conductivity σ of $\text{Li}_3\text{Sc}_2(\text{PO}_4)_3$ crystals was investigated in the frequency range from 5 Hz to $5 \cdot 10^5$ Hz [1, 2, 4]. The highest value of ionic conductivity of γ - $\text{Li}_3\text{Sc}_2(\text{PO}_4)_3$ single crystals was observed along the \vec{c} axis and at $T = 600$ K was found to be $\sigma = 3.0$ S/m (activation

energy $\Delta E = 0.38$ eV) [2]. The temperature of the phase transitions, the values of σ and ΔE are sensitive to the isomorphous substitutions $\text{Sc} \rightarrow \text{Fe}$ in the $\text{Li}_3\text{Fe}_x\text{Sc}_{2-x}(\text{PO}_4)_3$ quasibinary system. As it was shown in Refs. [1, 5] the lithium subsystem in the quasibinary system remains disordered down to room temperature for $0.2 \geq x \geq 0.6$. In temperature range from 293 to 600 K the value of ionic conductivity of the system is higher than that of $\text{Li}_3\text{Sc}_2(\text{Fe}_2)(\text{PO}_4)_3$ crystals. Since Li^+ -ion conductors have appeared as attractive materials for applications in CO_2 gas sensors and solid electrolyte batteries, the detection of the influence of the isomorphous substitutions of Sc^{3+} by another three-valence ion on the values of σ and ΔE of $\text{Li}_3\text{Sc}_2(\text{PO}_4)_3$ compounds stimulates further research of this phenomena. Our intention was to investigate the influence of substitution of Sc^{3+} by a comparatively small B^{3+} cation. We report the technological conditions of synthesis of the new compound $\text{Li}_3\text{B}_x\text{Sc}_{2-x}(\text{PO}_4)_3$ powders with $x = 0-2$, preparation of the glass samples, sintering of the ceramics, and results of our investi-

* The report presented at the 36th Lithuanian National Physics Conference, 16–18 June 2005, Vilnius, Lithuania.

gation of structure, surface, and electrical properties of the materials.

2. Experimental

Powdered compounds $\text{Li}_3\text{Sc}_{2-x}\text{B}_x(\text{PO}_4)_3$ at $x = 0$ –2 have been synthesized by subjecting to a solid phase reaction the stoichiometric mixtures of Li_2CO_3 (purity 99.999%), Sc_2O_3 (purity 99.999%), extra pure $\text{NH}_4\text{H}_2\text{PO}_4$, and H_3BO_3 . Each mixture was milled for 8 h in an agate planetary mill in ethyl alcohol, heated for 20 h at temperature $T = 723$ K, and milled for 12 h in the planetary mill. The synthesis continued with the sequence of heating for 2 h at $T = 1273$ K and milling in the planetary mill for 8 h. The fine powder was dried at $T = 393$ K for 24 h.

The powder was uniaxially cold pressed at 300 MPa. Ceramic pellets were sintered in air for 1 h. The sintering temperatures of $\text{Li}_3\text{Sc}_2(\text{PO}_4)_3$, $\text{Li}_3\text{Sc}_{1.5}\text{B}_{0.5}(\text{PO}_4)_3$, and $\text{Li}_3\text{ScB}(\text{PO}_4)_3$ ceramic samples were 1643, 1043, and 1023 K, respectively. The liquid phase of $\text{Li}_3\text{B}_2(\text{PO}_4)_3$ compound (the liquid phase temperature was found to be $T = 1273$ K) was air-quenched with a cooling rate of about 300 degree/min. The $\text{Li}_3\text{B}_2(\text{PO}_4)_3$ sample fabricated in this way was a single-phase glass. The structure parameters were analyzed at room temperature using diffraction of $\text{Cu } K_{\alpha 1}$ radiation from powder in the 2Θ region from 10 to 80 degrees with a step scan of 1 degree/min.

The studies of surfaces of the ceramic samples were carried out by the scanning electron microscope (SEM) 960 DSM. The measurements of complex conductivity $\tilde{\sigma} = \sigma' + i\sigma''$, complex impedance $\tilde{Z} = Z' + iZ''$, and complex dielectric permittivity $\tilde{\epsilon} = \epsilon' + i\epsilon''$ were performed by coaxial impedance spectrometer set-up in the frequency range from 10^6 to $1.2 \cdot 10^9$ Hz [6].

3. Results and discussion

The results of X-ray diffraction studies have shown that $\text{Li}_3\text{Sc}_{2-x}\text{B}_x(\text{PO}_4)_3$ at $x = 0, 0.5$, and 1 are mainly single-phase materials. A small amount of AlPO_4 was

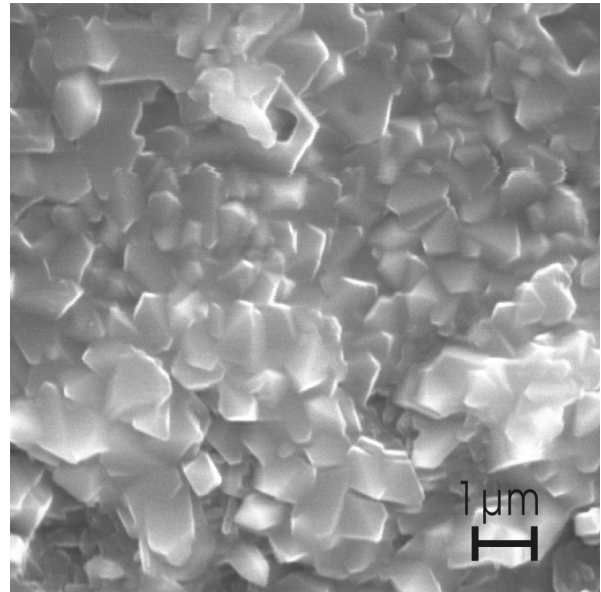


Fig. 1. SEM image of $\text{Li}_3\text{Sc}_{1.5}\text{B}_{0.5}(\text{PO}_4)_3$ surface.

detected in samples as impurities from the material of crucible. These compounds belong to the monoclinic crystallographic system (s. g. $P2_1/n$) with $z = 4$ formula units in the unit cell. The results of X-ray investigations revealed changes in the interplanar distances with change of x in these compounds. The lattice parameters, unit cell volume, and density of the materials are presented in Table 1.

The density of ceramic samples was found to be from 86 to 92% of the theoretical density of these materials. The results of investigation by SEM showed the presence of numerous microcracks on the surface of ceramic specimens. The characteristic image of SEM of $\text{Li}_3\text{Sc}_{1.5}\text{B}_{0.5}(\text{PO}_4)_3$ ceramic surface is shown in Fig. 1. The grains of ceramic samples sintered for 1 h have the sizes in the range from 300 to 700 nm. The results of investigation of the element composition of studied ceramics are shown in Table 2.

The temperature dependence of electric conductivity was derived from the impedance spectra measured at different temperatures. The results of measurements of the frequency dependences of Z'' and σ' show that the impedance spectra consist of two overlapping dispersion regions. Both processes are related to the ion

Table 1. Cell parameters and densities of the $\text{Li}_3\text{Sc}_{2-x}\text{B}_x(\text{PO}_4)_3$ compounds at $T = 300$ K.

Compounds	Lattice parameters, Å			Unit cell volume, Å ³	Density, g/cm ³
	<i>a</i>	<i>b</i>	<i>c</i>		
$\text{Li}_3\text{Sc}_2(\text{PO}_4)_3$	8.853(2)	12.273(2)	8.802(2)	956.36	2.747
$\text{Li}_3\text{Sc}_{1.5}\text{B}_{0.5}(\text{PO}_4)_3$	8.858(3)	12.290(3)	8.810(3)	959.17	2.619
$\text{Li}_3\text{ScB}(\text{PO}_4)_3$	8.849(1)	12.281(3)	8.799(1)	956.22	2.510
$\text{Li}_3\text{B}_2(\text{PO}_4)_3$	glass				

Table 2. The element compositions on the surface of $\text{Li}_3\text{Sc}_{2-x}\text{B}_x(\text{PO}_4)_3$ ceramics.

Compound	Elements, wt %					
	P	O	B	Al	Li	Sc
$\text{Li}_3\text{Sc}_2(\text{PO}_4)_3$	23.49	48.53	–	–	5.26	22.73
$\text{Li}_3\text{Sc}_{1.5}\text{B}_{0.5}(\text{PO}_4)_3$	24.55	50.72	1.43	2.72	5.50	17.81
$\text{Li}_3\text{ScB}(\text{PO}_4)_3$	25.70	53.11	2.99	3.23	5.76	12.44
$\text{Li}_3\text{B}_2(\text{PO}_4)_3$	28.39	58.65	6.61	3.00	6.36	–

transport within grains and in grain boundaries of the ceramic samples. The dispersion processes are thermally activated and shift towards higher frequencies with the increase in temperature. This shows that both dispersions have typical relaxation character. The observed relaxation dispersions can be analyzed using the frequency dependences of ac impedance in the complex plane.

As an example, the complex plane impedance plots of $\text{Li}_3\text{Sc}_{1.5}\text{B}_{0.5}(\text{PO}_4)_3$ ceramic sample at different temperatures are shown in Fig. 2. The plot consists of two overlapping semicircles with centres below the Z' axis. The relaxation processes within grains are responsible for the high frequency arc, and the relaxation processes in the grain boundaries of the ceramic samples are responsible for the low frequency arc.

With the increase in temperature the relaxation dispersion frequency range related to the processes within grains of the ceramics gradually moves out from the investigated frequency range. The values of the intra-grain conductivity σ_g and total conductivity σ_{tot} were obtained from the dependences $Z''(Z')$ and $\sigma''(\sigma')$ at different temperatures. The temperature dependences of σ_g and σ_{tot} are shown in Figs. 3 and 4, respectively. The activation energies of σ_g and σ_{tot} were calculated according to Arrhenius equation

$$\sigma_{g,\text{tot}} = \frac{\sigma_0}{T} \exp\left(\frac{\Delta E_{g,\text{tot}}}{kT}\right), \quad (1)$$

where $k = 1.38 \cdot 10^{-23} \text{ J}\cdot\text{K}^{-1}$ is Boltzmann constant. The $\sigma_g(T)$ dependence of $\text{Li}_3\text{Sc}_2(\text{PO}_4)_3$ in Fig. 3 can be divided into four regions: below 450 K, from 450 to 470 K, from 470 to 530 K, and above 530 K. According to the structural analysis results for $\text{Li}_3\text{Sc}_2(\text{PO}_4)_3$ crystals [2], the anomalies of σ_g in temperature ranges 450 – 470 K and 470 – 530 K can be caused by the $\alpha \leftrightarrow \beta$ and $\beta \leftrightarrow \gamma$ phase transitions in the investigated compounds.

The results of investigation of $\sigma_{g,\text{tot}}(T)$ have revealed that the isomorphous substitution $\text{Sc} \rightarrow \text{B}$ leads to the changes of temperature T_γ of phase transitions to the γ - $\text{Li}_3\text{B}_x\text{Sc}_{2-x}(\text{PO}_4)_3$ phase and also influences the values of σ_g and σ_{tot} as well as their activation ener-

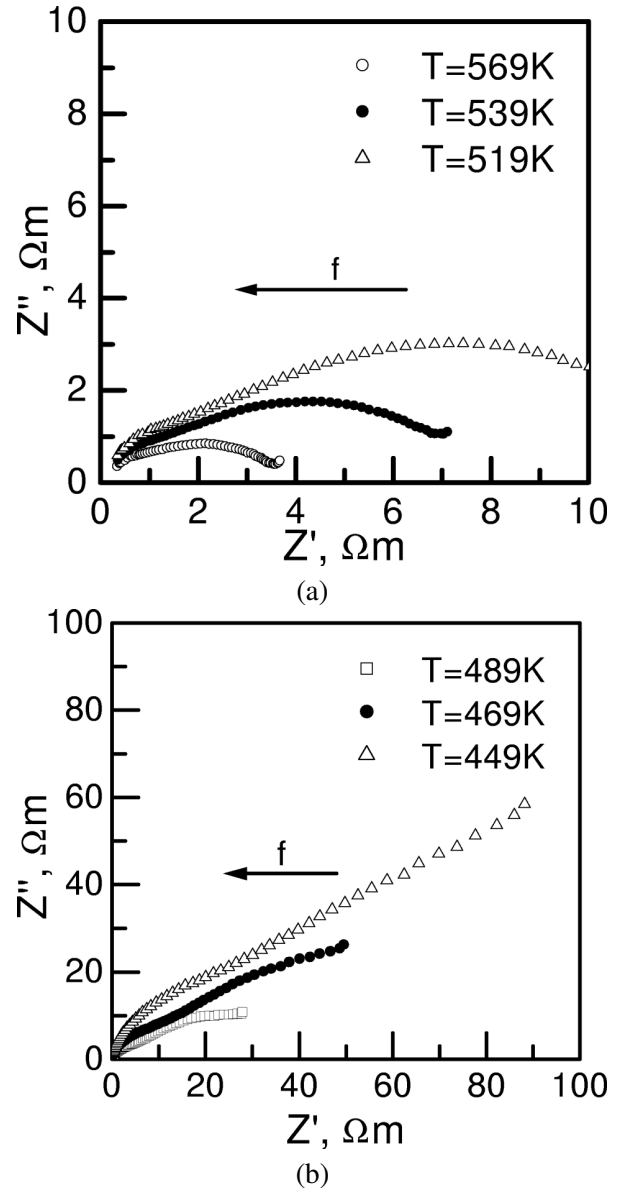


Fig. 2. Impedance spectra of $\text{Li}_3\text{Sc}_{1.5}\text{B}_{0.5}(\text{PO}_4)_3$ ceramics at different temperatures.

gies. The increase of the stoichiometric factor x caused the increase of σ_g and decrease of σ_{tot} , ΔE_g , ΔE_{tot} in the low temperature region, while in the γ -phase it caused the decrease of both σ_g and σ_{tot} . The value of σ_{tot} of $\text{Li}_3\text{B}_2(\text{PO}_4)_3$ glass samples at low temperature is higher than the value of σ_g of α - $\text{Li}_3\text{Sc}_2(\text{PO}_4)_3$

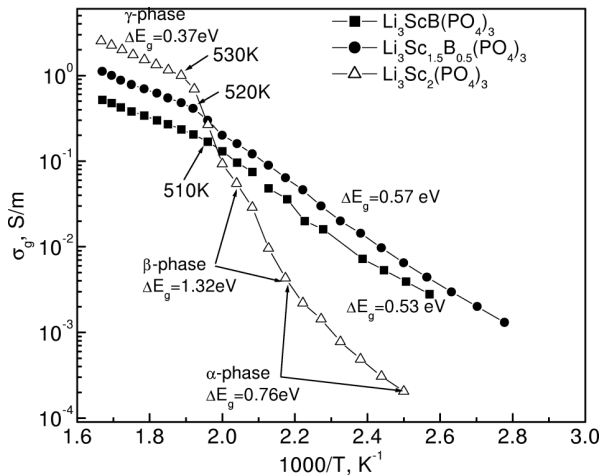
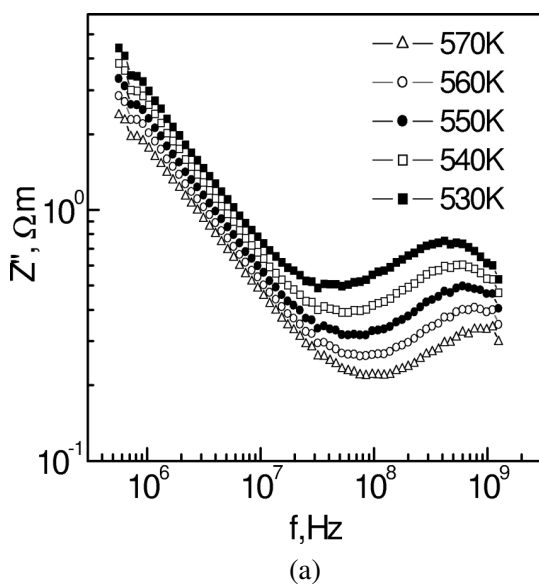


Fig. 3. Temperature dependences of intragrain conductivity of $\text{Li}_3\text{Sc}_{2-x}\text{B}_x(\text{PO}_4)_3$ ceramics at $x = 0, 0.5,$ and 1 .

compound. The temperatures of γ -phase transitions decrease with the increase of x . The temperatures of γ -phase transitions for the compounds with stoichiometric factor $x = 0, 0.5,$ and 1 are around $530, 520,$ and 510 K, respectively. The anomalies of σ_g at $\alpha \leftrightarrow \beta$ phase transition were not detected in the compounds with stoichiometric factor $x = 0.5$ and 1 . The values of $\sigma_g, \sigma_{\text{tot}}, \Delta E_g,$ and ΔE_{tot} of the investigated compounds are listed in Table 3. The relaxation frequency of the intragrain processes in ceramic samples was obtained from the maximum of frequency dependence of Z'' at different temperatures. The characteristic frequency dependences of Z'' for $\text{Li}_3\text{Sc}_2(\text{PO}_4)_3$ and the inverse temperature dependences of the σ_g relaxation frequencies are shown in Fig. 5. The relaxation fre-



(a)

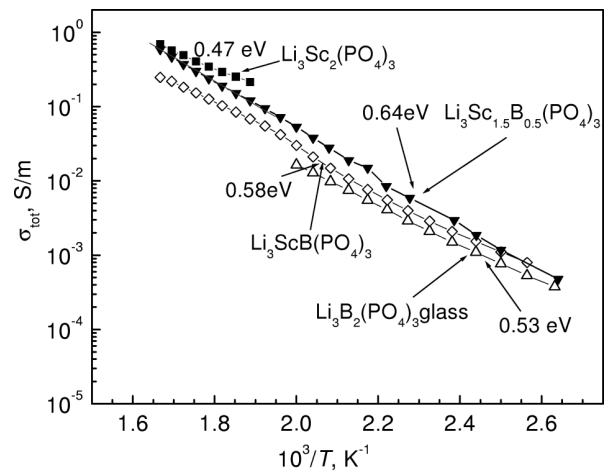
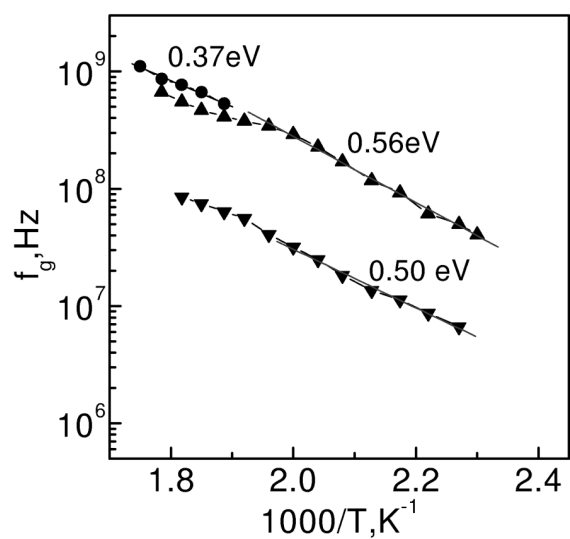


Fig. 4. Temperature dependences of total conductivity of $\text{Li}_3\text{Sc}_{2-x}\text{B}_x(\text{PO}_4)_3$ ceramic at $x = 0, 0.5,$ and 1 and of $\text{Li}_3\text{B}_2(\text{PO}_4)_3$ glass samples.

quencies within the grains of ceramic samples increase with temperature according to the formula

$$f_g = f_0 \exp\left(\frac{\Delta E_f}{kT}\right), \quad (2)$$

where f_0 is an attempt frequency related to the lattice vibrations and E_f is the activation energy of f_g . The comparison of the estimated values of ΔE_g and ΔE_f shows that these energies are approximately equal for the same compound. Since we have found that the activation energies of intragrain ionic conductivity of the investigated ceramic samples are equal to the activation energies of relaxation frequency, which can be attributed to the migration of Li^+ , the concentration of charge carriers remains constant with temperature.

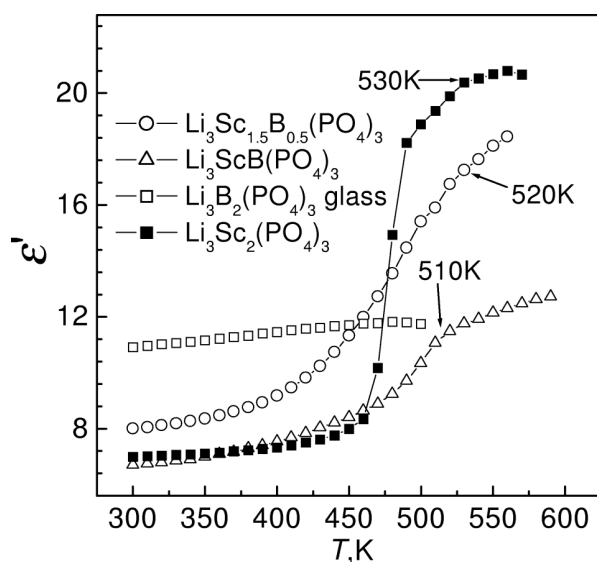


(b)

Fig. 5. (a) Frequency dependences of Z'' of $\gamma\text{-Li}_3\text{Sc}_2(\text{PO}_4)_3$ compound at different temperatures. (b) Temperature dependences of the relaxation frequency of the dispersion σ_g of $\text{Li}_3\text{Sc}_{2-x}\text{B}_x(\text{PO}_4)_3$ ceramics at $x = 0, 0.5,$ and 1 .

Table 3. Values of σ_g , σ_{tot} , ΔE_g , ΔE_{tot} of $\text{Li}_3\text{Sc}_{2-x}\text{B}_x(\text{PO}_4)_3$ ceramics at different temperatures.

T , K	Stoichiometric factor x	σ_g , S/m	ΔE_g , eV	σ_{tot} , S/m	ΔE_{tot} , eV
400	0	$1.99 \cdot 10^{-4}$	0.76	–	–
	0.5	$6.5 \cdot 10^{-3}$	0.57	$1.2 \cdot 10^{-3}$	0.64
	1	$3.93 \cdot 10^{-3}$	0.53	$1.18 \cdot 10^{-3}$	0.59
	2 (glass)	–	–	$7.7 \cdot 10^{-4}$	0.53
460	0	$4.3 \cdot 10^{-3}$	1.32	–	–
	0.5	0.064	0.57	$11.5 \cdot 10^{-2}$	0.64
	1	0.36	0.53	$7.68 \cdot 10^{-3}$	0.59
	2	–	–	$5.5 \cdot 10^{-3}$	0.53
540	0	1.15	0.37	0.25	0.47
	0.5	0.545	–	0.15	–
	1	0.27	–	0.085	–
	2	–	–	–	–

Fig. 6. Temperature dependences of dielectric permittivity of $\text{Li}_3\text{Sc}_x\text{B}_{2-x}(\text{PO}_4)_3$ ceramic at $x = 0, 0.5$, and 1 and of $\text{Li}_3\text{B}_2(\text{PO}_4)_3$ glass samples.

Such ion transport peculiarities are characteristic for oxygen vacancy [7, 8], Na^+ [9], and Li^+ [10, 11] solid electrolytes.

Temperature dependences of the real part of complex dielectric permittivity ϵ' of $\text{Li}_3\text{Sc}_{2-x}\text{B}_x(\text{PO}_4)_3$ compounds are shown in Fig. 6. The dielectric permittivity was obtained at the electric field frequency of 1 GHz. The values of ϵ' at 300 K were found to be $\epsilon' = 7$ for $\text{Li}_3\text{Sc}_2(\text{PO}_4)_3$ and $\text{Li}_3\text{ScB}(\text{PO}_4)_3$ compounds, $\epsilon' = 8$ for $\text{Li}_3\text{Sc}_{1.5}\text{B}_{0.5}(\text{PO}_4)_3$ compound, and $\epsilon' = 11$ for $\text{Li}_3\text{B}_2(\text{PO}_4)_3$ glass. The $\alpha \leftrightarrow \beta$ and $\beta \leftrightarrow \gamma$ phase transitions in $\text{Li}_3\text{Sc}_2(\text{PO}_4)_3$ compounds can be seen as anomalies of ϵ' . In the compounds with $x = 0.5$ and 1 the anomalies of ϵ' were detected at 520 and 510 K temperatures, respectively. The activation en-

ergies of σ_g and σ_{tot} of these compounds also suffer the changes at exactly the same temperatures (Figs. 3, 4). In the γ -phase the value of ϵ' can be related to the contribution of polarization due to Li^+ migration, vibrations of lattice, and electronic polarization.

4. Conclusions

The solid electrolyte $\text{Li}_3\text{Sc}_{2-x}\text{B}_x(\text{PO}_4)_3$ compounds at $x = 0-2$ have been synthesized by solid state reaction and studied by X-ray powder diffraction. The surface of the ceramic samples was investigated by SEM. The electrical properties of the ceramics and $\text{Li}_3\text{B}_2(\text{PO}_4)_3$ glass samples were carried out in the frequency range $10^6-1.2 \cdot 10^9$ Hz and in the temperature range 300–600 K. Two regions of relaxation dispersion of the conductivity were found in the ceramics. The dispersions are caused by fast Li^+ ion transport in the bulk and in the grain boundaries of the ceramics. Isomorphic substitution $\text{Sc} \rightarrow \text{B}$ leads to the changes of temperature of phase transition to the γ - $\text{Li}_3\text{Sc}_{2-x}\text{B}_x(\text{PO}_4)_3$ phase. The increase of stoichiometric factor x causes the increase of σ_g values and the decrease of σ_{tot} and activation energies of the conductivities in the temperature region below T_γ , but the decrease of both σ_g and σ_{tot} in the γ -phase. The temperature dependences of the bulk conductivity and relaxation frequency in the grains of γ -phase give the same value of the activation energy. This suggests that fast Li^+ ion transport in the grains of γ - $\text{Li}_3\text{Sc}_{2-x}\text{B}_x(\text{PO}_4)_3$ compounds may be described by the temperature dependent mobility, while the concentration of mobile ions remains constant with temperature. The increase of x leads to the increase of ϵ' at the frequency of external electrical field of 1 GHz. The

values of ε' at room temperature are related to the contribution of migration of Li^+ ions, lattice vibrations, and electronic polarization.

Acknowledgement

This work was supported by the Lithuanian State Science and Studies Foundation.

References

- [1] S. Sigaryov, V.G. Terziev, and J.L. Dorman, *Phys. Rev. B* **49**, 6319 (1994).
- [2] A.B. Bykov, A.P. Chirkin, L.N. Demyanets, S.N. Doronin, E.A. Genkina, A.K. Ivanov-Shits, I.P. Kondratyuk, B.A. Maksimov, O.K. Melnikov, L.N. Muradyan, V.I. Simonov, and V.A. Timofeeva, *Solid State Ionics* **38**, 31 (1990).
- [3] S.E. Sigaryov, *Kristallografiya* (in Russian) **37**, 1005 (1992).
- [4] S.E. Sigaryov, *Solid State Commun.* **75**, 1005 (1990).
- [5] A. Dindune, A. Kežionis, J. Ronis, Z. Kanepė, R. Sobiestianskas, E. Kazakevičius, and A. Orliukas, in: *Proceedings of the 2nd International Conference of DAAAM, Tallinn, Estonia, 27–29 April 2000*, pp. 179–182.
- [6] R. Sobiestianskas, A. Dindune, Z. Kanepė, J. Ronis, A. Kežionis, E. Kazakevičius, and A. Orliukas, *Mat. Sci. Eng. B* **76**, 184 (2000).
- [7] A. Orliukas, P. Bohac, K. Sasaki, and L. Gauckler, *J. Eur. Ceram. Soc.* **12**, 87 (1993).
- [8] A. Kežionis, W. Bogusz, F. Krok, J. Dygas, A. Orliukas, I. Abrahams, and W. Gembicki, *Solid State Ionics* **119**, 145 (1999).
- [9] W. Bogusz, J. Dygas, F. Krok, A. Kežionis, R. Sobiestianskas, E. Kazakevičius, and A. Orliukas, *Phys. Status Solidi* **183**, 323 (2001).
- [10] A. Dindune, E. Kazakevičius, Z. Kanepė, J. Ronis, A. Kežionis, and A. Orliukas, *Phosphorus Research Bulletin* **13**, 107 (2002).
- [11] A. Orliukas, A. Dindune, Z. Kanepė, J. Ronis, E. Kazakevičius, and A. Kežionis, *Solid State Ionics* **157**, 177 (2003).

$\text{Li}_3\text{Sc}_{2-x}\text{B}_x(\text{PO}_4)_3$ SUPERJONIKŲ GAMYBA IR JŲ ELEKTRINĖS SAVYBĖS

T. Šalkus^a, E. Kazakevičius^a, V. Kunigėlis^a, L. Jucius^a, A. Dindune^b, Z. Kanepė^b, J. Ronis^b, A. Kežionis^a, B. Bleiber^d, H.-J. Lang^c, A.F. Orliukas^a

^a *Vilniaus universitetas, Vilnius, Lietuva*

^b *Rygos technikos universiteto Neorganinės chemijos institutas, Salaspilis, Latvija*

^c *Freibergo kasybos ir technologijos universiteto Keraminių medžiagų institutas, Freibergas, Vokietija*

^d *Freibergo kasybos ir technologijos universiteto Metalurgijos institutas, Freibergas, Vokietija*

Santrauka

Pateiktos technologinės superjoninių $\text{Li}_3\text{Sc}_{2-x}\text{B}_x(\text{PO}_4)_3$ (čia $x = 0 - 2$) medžiagų sintezės sąlygos, jų rentgenostruktūrinių ir elementinės sudėties tyrimų rezultatai. Pagaminus $\text{Li}_3\text{Sc}_2(\text{PO}_4)_3$, $\text{Li}_3\text{Sc}_{1,5}\text{B}_{0,5}(\text{PO}_4)_3$ ir $\text{Li}_3\text{ScB}(\text{PO}_4)_3$ junginių keramikas bei $\text{Li}_3\text{B}_2(\text{PO}_4)_3$ stiklą, jų paviršiaus mikrosandara buvo tirta skenuojančiu elektroniniu mikroskopu. Elektrinės junginių savybės buvo tirtos $10^6 - 1,2 \cdot 10^9$ Hz elektrinio lauko bei 300 – 600 K temperatūros intervaluose. $\text{Li}_3\text{Sc}_2(\text{PO}_4)_3$ keramikose 450 – 480 K ir 500 – 535 K temperatūros intervaluose vyksta atitinkamai $\alpha \leftrightarrow \beta$ ir $\beta \leftrightarrow \gamma$ faziniai virsmai, kurių metu reiškiasi laidumo ir dielektrinės skvarbos anomalijos. Nustatyta, kad stochiometrijos faktoriaus x didėjimas žemina fazinio virsmo į junginių superjoninę γ fazę

temperatūrą T_γ . Tirtose keramikose aptiktos dvi relaksacinio tipo dispersijos, susijusios su Li^+ jonų pernaša kristalituose ir tarpkristalitinėse terpėse. Be to, didėjant x , esant žemesnei už T_γ temperatūrai, didėja keramikų kristalitinis (σ_g) ir bendrasis (σ_{tot}) laidumai, o jų aktyvacijos energijos mažėja. Parodyta, kad šiose medžiagose judriųjų Li^+ jonų tankis kristalituose nepriklauso nuo temperatūros, o kristalitinio laidumo temperatūrinį kitimą lemia jonų judrio temperatūrinė kaita. Pateiktos tirtųjų keramikų ir $\text{Li}_3\text{B}_2(\text{PO}_4)_3$ stiklo santykinės dielektrinės skvarbos ε' , išmatuotos 1 GHz dažnio elektriniame lauke, temperatūrinės priklausomybės. Tų keramikų kristalitų dielektrinės skvarbos vertės lemia tiek migracinės, tampriosios joninės, elektroninės poliarizacijų indėliai, tiek ir stochiometrijos faktoriaus x didumas.